The adaptations are minor. The first step of the sequence for Co(III) takes place with OH^- as the entering nucleophile; with Ru(III), H_2O suffices to hydrolyze the nitrile. Linkage isomerization, as in the second step, is expected to be more rapid for Ru(III) than for Co(III). It is so rapid that the intermediate $(NH_3)_5Ru(2\text{-}X)^{3+}$, where X is carboxamidocyanobenzene, is not observed at high acidity.

As the last point to be raised in the discussion we draw attention to the significantly lower intensity of the nitrile stretching frequency when the ligand is associated with Ru(III) than when associated with Co(III).[25] The conclusion as stated, which is based on observations with the mononuclear complexes, where the unencumbered nitriles serve as internal standards, as well as with the binuclear complexes, seems dependable. There are consistent differences also in the frequency shifts. We suggest that the differences are ascribable to the differences in electronic structure: πd^5 for Ru(III) and π^6 for Co(III). The vacancy in a low-lying orbital for the former, but not for the latter, leads to greater ligand-to-metal charge transfer for Ru(III). This effect has been invoked to account for the greater efficacy of Ru(III) compared to Co(III) in promoting nitrile hydrolysis and may be the cause of differences in the intensities of the IR frequencies. In the absence of a firm theoretical basis for the correlation offered, the suggestion is of course to be regarded as tentative.

(25) Kupferschmidt, W. C.; Jordan, R. B. *Inorg. Chem.* **1982**, *21*, 2089. Herein is reported that for both the fumaronitrile and malononitrile complexes of pentaamminecobalt(III), the intensity of the nitrile stretch in the IR for the metal-bound nitrile is higher than that of the free nitrile.

Acknowledgment. Support by the National Institutes of Health (Grant GM13638) is gratefully acknowledged, as are helpful discussions with Arden Johnson of the data on IR intensities. Gratefully acknowledged as well is the leadership of R. A. Marcus in contributing to providing the theoretical framework that has made a science of the kind of work reported here. Henry Taube expresses his appreciation for the continued interest R. A. Marcus has shown in new experimental results and Dr. Marcus's unfailing tact in helping him to understand their significance.

Registry No. I, 102575-67-7; I^{5+}, 102575-77-9; II, 102575-69-9; II^{5+}, 102575-78-0; III, 102575-71-3; III^{5+}, 102575-79-1; $[(NH_3)_5Co(1,4\text{-dcb})](TFMS)_3$, 102575-72-4; $[(NH_3)_5Co(TFMS)](TFMS)_2$, 75522-50-8; $[(NH_3)_5Ru(TFMS)](TFMS)_2$, 84278-98-8; $[(NH_3)_5Co(1,3\text{-dcb})](TFMS)_3$, 102575-73-5; $[(NH_3)_5Co(1,2\text{-dcb})](TFMS)_3$, 102575-74-6; $[(NH_3)_5Ru(1,4\text{-dcb})](TFMS)_3$, 90245-43-5; $[(NH_3)_5Ru(1,3\text{-dcb})](TFMS)_3$, 90245-42-4; $[(NH_3)_5Ru(1,2\text{-dcb})](TFMS)_3$, 90245-41-3; $[(NH_3)_5Ru(1,4\text{-dcb})]^{2+}$, 46739-38-2; $[(NH_3)_5Ru(1,3\text{-dcb})]^{2+}$, 46737-88-6; $[(NH_3)_5Ru(1,2\text{-dcb})]^{2+}$, 102575-76-8.

Distance, Stereoelectronic Effects, and the Marcus Inverted Region in Intramolecular Electron Transfer in Organic Radical Anions[1]

G. L. Closs,*†‡ L. T. Calcaterra,†‡ N. J. Green,† K. W. Penfield,‡ and J. R. Miller*‡

Department of Chemistry, The University of Chicago, Chicago, Illinois 60637, and Argonne National Laboratory, Argonne, Illinois 60439 *(Received: January 14, 1986; In Final Form: March 12, 1986)*

A series of molecules with the general structure A_1–Sp–A_2 have been synthesized. Pulse radiolysis was used to convert them into negative ions, and the rates of intramolecular electron transfer were measured. In the first series studied Sp is the androstane skeleton with the acceptors attached to the 3- and 16-positions. The series consisted of eight molecules with A_2 = 4-biphenyl and eight different A_1 groups differing in electron affinity by 2.4 eV. The electron transfer rates differ by more than 3 orders of magnitude throughout the series and depend in a very nonlinear fashion on the free energy of the reaction. The rate–free energy profile reaches a maximum in methyltetrahydrofuran at approximately 1-eV exoergicity. At more negative free energies the rates fall off substantially, showing the existence of an "inverted region". In isooctane the rate maximum occurs at less exoergic reactions. The second series of molecules was designed to study the effect of the spacer which was varied from the steroid to decalins (eight compounds) and cyclohexanes (four compounds). No comprehensive distance dependence exists. Instead, the rates are strongly influenced by the donor–acceptor attachment geometry which influences the electronic coupling. This strong dependence on stereochemistry suggests that the major component of the coupling occurs through bonds. A semiquantitative relationship for the magnitude of this coupling with the number of bonds intervening between donor and acceptor was established. For the type of spacers studied it was found that the electron transfer rates are slowed down by 1 order of magnitude for each 2.0 bonds for a constant reorganization energy. This relationship is shown to hold only if the attachment stereochemistry throughout the series whose members are compared is held constant. The stereoelectronic effects are of substantial magnitude and are predicted to be very large in some special structures.

Introduction

A number of years ago we initiated a collaborative research program between Argonne National Laboratory and The University of Chicago aimed at elucidating some of the intricacies of intramolecular long-distance electron transfer (LDET). Not too long ago "conventional wisdom" held the view that electron transfer (ET) between molecules required a proximity of electron donor (D) and acceptor (A) comparable to their van der Waals radii. Recent work by us and others has laid this myth to rest and has convincingly demonstrated that LDET not only exists but can be remarkably fast.[2-57] Long-distance electron transfer has been studied in several systems in which D and A have been kept apart by a rigid spacer group[2-22] or by incorporating them in rigid

† University of Chicago.
‡ Argonne National Laboratory.

(1) Work supported by the Office of Basic Energy Sciences, Division of Chemical Science, US-DOE, under Contract No. W-31-109-ENG-38 and the National Science Foundation under Grant No. CHE-8218164.
(2) Calcaterra, L. T.; Closs, G. L.; Miller, J. R. *J. Am. Chem. Soc.* **1983**, *105*, 670.
(3) Miller, J. R.; Calcaterra, L. T.; Closs, G. L. *J. Am. Chem. Soc.* **1984**, *106*, 3047.
(4) Mazur, S.; Dixit, V. M.; Gerson, F. *J. Am. Chem. Soc.* **1980**, *102*, 5343.
(5) Passman, P.; Verhoeven, J. W.; De Boer, Th. *Chem. Phys. Lett.* **1978**, *59*, 381.
(6) Passman, P.; Koper, N. W.; Verhoeven, J. W. *Recl.: J. R. Neth. Chem. Soc.* **1983**, *102*, 55.

0022-3654/86/2090-3673$01.50/0

TABLE I: Rate Constants[a,e] for Intra- and Intermolecular Electron Transfer in Anions of Bifunctional Steroids A_x–Sp–Bi^- (Bi = 4-Biphenylyl) at T = 296 K

		MTHF		isooctane	
acceptor group (A_x)	$-\Delta G°$, eV	k_{intra}, s^{-1}	k_{inter}[a], 10^9 M^{-1} s^{-1}	k_{intra}, s^{-1}	k_{inter},[a] 10^9 M^{-1} s^{-1}
4-biphenylyl	0	$(5.6 \times 10^5$[b]		$1 \times 10^9 <<$ mtb[b]	
2-naphthyl[e]	0.05[c]	$(1.5 \pm 0.5) \times 10^6$	5.7	$(1.5 \pm 0.5) \times 10^9$	6.7
9-phenanthryl	0.16[c]	$(1.25 \pm 0.2) \times 10^7$	7.0	$>2 \times 10^9$	13.9
1-pyrenyl	0.52[d]	$(1.5 \pm 0.5) \times 10^9$	12.0	$>2 \times 10^9$	13.5
2-(5,8,9,10-tetrahydronaphthoquinonyl)	1.23[d]	$>2 \times 10^9$	11.1	$(1.0 \pm 0.5) \times 10^9$	12.9
2-naphthoquinonyl	1.93[d]	$(3.8 \pm 1) \times 10^8$	9.9 ± 1	$>2 \times 10^9$	17.1
2-benzoquinonyl	2.10[d]	$(2.5 \pm 0.3) \times 10^8$	6.2	$(3.6 \pm 0.8) \times 10^6$	10.9
2-(5-chlorobenzoquinonyl)	2.29[d]	$(1.7 \pm 0.2) \times 10^8$	4.4	$(3.5 \pm 0.5) \times 10^6$	9.5
2-(5,6-dichlorobenzoquinonyl)	2.40[d]	$(7 \pm 3) \times 10^7$	3.0 ± 1	$(1.4 \pm 0.25) \times 10^8$	9.8

[a] Uncertainties ±15% (1 standard deviation) unless noted otherwise. [b] The rates of the exchange reactions in Bi^-–Sp–Bi were *not* measured but were estimated by extrapolating from measured data. [c] From equilibria measured by pulse radiolysis. [d] Estimated from redox potentials in DMF (ref 2). [e] The forward rate constant is reported. The rate of approach to equilibrium is $k_f + k_r$.

glasses or polymers.[23-31] Use has been made of monolayer assemblies[32-34] and proteins[35-42] to accomplish the same purpose. Recent crystallographic work[43,44] and kinetic measurements[44,57] on photosynthetic reaction centers have shown that nature makes use of LDET in one of the most important processes known, photosynthesis.

Having thus justified that LDET does not only exist but is very important in biochemistry, one might ask why we have chosen to study *intra*molecular processes. The answer to that is based on the fact that *inter*molecular reactions suffer from the fact that the rates are determined by two processes, diffusion and electron transfer (ET). We hope it will become clear in this article that diffusion can mask ET to an extent that the most interesting features of ET never show up. In fact, some of these features were first demonstrated in rigid glassy matrices in which diffusion has been arrested.[23-31] Also, almost all biochemical ET processes are intramolecular if the protein complex is considered to be one molecule with fixed distances, although natural systems do not necessarily employ covalent bonding. Of course, our work is not the first to study intramolecular electron transfer; there have been many examples before. The new features we sought and achieved are well-defined, fixed, long distances with a range of energetics

(7) Passman, P. Ph.D. Thesis, University of Amsterdam, Amsterdam, The Netherlands, 1980.
(8) Moore, T. A.; Gust, D.; Mathis, P.; Mialocq, J.-C.; Chachaty, C.; Bensasson, R. V.; Land, E. J.; Doizi, D.; Liddell, P. A.; Lehman, W. R.; Nemeth, G. A.; Moore, A. L. *Nature (London)* **1984**, *307*, 630.
(9) Joran, A. D.; Leland, B. A.; Geller, G. G.; Hopfield, J. J.; Dervan, P. B. *J. Am. Chem. Soc.* **1984**, *106*, 6090.
(10) Wasielewski, M. R.; Niemczyk, M. P.; Svec, W. A.; Pewitt, E. B. *J. Am. Chem. Soc.* **1985**, *107*, 5562.
(11) Hush, N. S.; Paddon-Rowe, M. N.; Cotsans, E.; Overing, H.; Verhoeven, J. W. *Chem. Phys. Lett.* **1985**, *117*, 8.
(12) Fujita, I.; Fajer, J.; Chang, C.-K.; Wang, C. B.; Bergkamp, M. A.; Netzel, T. L. *J. Phys. Chem.* **1982**, *86*, 3754.
(13) Creutz, C.; Kroger, P.; Matsubara, T.; Netzel, T. L.; Sutin, N. *J. Am. Chem. Soc.* **1979**, *101*, 5442.
(14) Heitile, H.; Michel-Beyerle, M. E. In *Antennas and Reaction Centers of Photosynthetic Bacteria*; Michel-Beyerle, M. E., Ed.; Springer-Verlag: West Berlin, 1985; p 250.
(15) Lindsey, J. S.; Mauzerall, D. C.; Linschitz, H. *J. Am. Chem. Soc.* **1983**, *105*, 6528.
(16) Huddleston, R. K.; Miller, J. R. *J. Chem. Phys.* **1983**, *79*, 5337.
(17) Schmidt, J. A.; Siemiarczuk, A.; Weedon, A. C.; Bolton, J. R. *J. Am. Chem. Soc.* **1985**, *107*, 6112.
(18) Roach, K. J.; Weedon, A. C.; Bolton, J. R.; Connolly, J. S. *J. Am. Chem. Soc.* **1983**, *105*, 7224.
(19) (a) Bolton, J. R.; Ho, T.-F.; Liauw, S.; Siemiarczuk, A.; Wan, C. S. K.; Weedon, A. C. *J. Chem. Soc., Chem. Commun.* **1985**, 559. (b) Gonzalez, M. C.; McIntosh, A. R.; Bolton, J. R.; Weedon, A. C. *J. Chem. Soc., Chem. Commun.* **1984**, 1183.
(20) Isied, S. S. *Prog. Inorg. Chem.* **1984**, *32*, 443.
(21) Isied, S. S.; Vassilian, A. *J. Am. Chem. Soc.* **1984**, *106*, 1732.
(22) Mataga, N.; Karen, A.; Okada, T.; Nishitani, S.; Kurata, N.; Sakata, Y.; Misumi, S. *J. Phys. Chem.* **1984**, *88*, 5138.
(23) Miller, J. R.; Beitz, J. V.; Huddleston, R. K. *J. Am. Chem. Soc.* **1984**, *106*, 5057.
(24) Miller, J. R.; Beitz, J. V. *J. Chem. Phys.* **1981**, *74*, 6476; *J. Chem. Phys.* **1979**, *71*, 4579. The latter reference gives tables with references, as well as examples of the effect of excited states on rates.
(25) Miller, J. R. *Science* **1975**, *189*, 221.
(26) Miller, J. R.; Hartman, K.; Abrash, S. *J. Am. Chem. Soc.* **1982**, *104*, 4286.
(27) Zamaraev, K. I.; Khairutdinov, R. F. *Russ. Chem. Rev. (Engl. Transl.)* **1978**, *47*, 518.
(28) Guarr, T.; McGuire, M. E.; McLendon, G. *J. Am. Chem. Soc.* **1985**, *107*, 5104.
(29) Kira, A.; Imamura, M. *J. Phys. Chem.* **1984**, *88*, 1865.
(30) Kira, A. *J. Phys. Chem.* **1981**, *85*, 3047.
(31) Kira, A.; Nosaka, Y.; Imamura, M. *J. Phys. Chem.* **1980**, *84*, 1882.
(32) Kuhn, H. *Life Sci. Res. Rep.* **1979**, *12*, 151.
(33) Kuhn, H. *Pure Appl. Chem.* **1979**, *51*, 341.
(34) Mobius, D. *Acc. Chem. Res.* **1981**, *14*, 63.
(35) McLendon, G. L.; Winkler, J. R.; Nocera, D. G.; Mauk, M. R.; Mauk, A. G.; Gray, H. B. *J. Am. Chem. Soc.* **1985**, *107*, 739.
(36) Peterson-Kennedy, S. E.; McGourty, J. L.; Ho, P. S.; Sutoris, C. J.; Liang, N.; Zemel, H.; Blough, N. V.; Margoliash, E.; Hoffman, B. M. *Coord. Chem. Rev.* **1985**, *64*, 125.
(37) Faraggi, M.; Steiner, J. P.; Klapper, M. H. *Biochemistry* **1985**, *24*, 3273.
(38) Ho, P. S.; Sutoris, C.; Liang, N.; Margoliash, E.; Hoffman, B. M. *J. Am. Chem. Soc.* **1985**, *107*, 1070.
(39) Kleinfeld, D.; Okamura, M. Y.; Feher, G. *Biochim. Biophys. Acta* **1984**, *766*, 126.
(40) Simolo, K. P.; McLendon, G. L.; Mauk, M. R.; Mauk, A. G. *J. Am. Chem. Soc.* **1984**, *106*, 5012.
(41) Nocera, D. G.; Winkler, J. R.; Yocom, K. M.; Bordignon, E.; Gray, H. B. *J. Am. Chem. Soc.* **1984**, *106*, 5145.
(42) Isied, S. S.; Kuehn, C.; Worosila, G. *J. Am. Chem. Soc.* **1984**, *106*, 1722.
(43) Diesenhoffer, J.; Epp, O.; Miki, K.; Huber, R.; Michl, H. *Nature (London)* **1985**, *318*, 618; *J. Mol. Biol.* **1984**, *180*, 385.
(44) See several references in ref 14.
(45) Chance, B.; DeVault, D. In *Proceedings of the 5th Nobel Symposium*; Claeson, S., Ed.; Soendergarn: Stockholm, Sweden, 1967; p 21.
(46) Kirmaier, C.; Holten, D.; Parson, W. W. *Biochim. Biophys. Acta* **1985**, *810*, 49.
(47) Kirmaier, C.; Holten, D.; Parson, W. W. *Biochim. Biophys. Acta* **1985**, *810*, 33.
(48) Popovic, Z. D.; Kovacs, G. J.; Vincett, P. S.; Dutton, P. L. *Chem. Phys. Lett.* **1985**, *116*, 405.
(49) Moehl, K. W.; Lous, E. J.; Hoff, A. J. *Chem. Phys. Lett.* **1985**, *121*, 22.
(50) Kleinfeld, D.; Okamura, M. Y.; Feher, G. *Biophys. J.* **1985**, *48*, 849.
(51) Kleinfeld, D.; Okamura, M. Y.; Feher, G. *Biochim. Biophys. Acta* **1984**, *766*, 126.
(52) Boxer, S. G.; Chidsey, C. E. D.; Roelofs, M. G. *Annu. Rev. Phys. Chem.* **1983**, *34*, 389.
(53) Wasielewski, M. R.; Bock, C. H.; Bowman, M. K.; Norris, J. R. *J. Am. Chem. Soc.* **1983**, *105*, 2903.
(54) Boxer, S. G.; Chidsey, C. E. D.; Roelofs, M. G. *J. Am. Chem. Soc.* **1982**, *104*, 1452.
(55) Boxer, S. G.; Chidsey, C. E. D.; Roelofs, M. G. *J. Am. Chem. Soc.* **1982**, *104*, 2674.
(56) Arata, H.; Parson, W. W. *Biochim. Biophys. Acta* **1981**, *638*, 201.
(57) Bowman, M. K.; Budil, D. E.; Closs, G. L.; Kostka, A. G.; Wraight, C. A.; Norris, J. R. *Proc. Natl. Acad. Sci. U.S.A.* **1981**, *78*, 3305.

sufficient to study nuclear reorganization energies. While flexible spacer groups are much easier to make than rigid ones, we wanted to avoid uncertainties in donor–acceptor distances. After a preliminary communication describing part of our work had appeared in print, a number of papers describing results obtained on rigid systems have been published, and most results support our original conclusions.[8-22]

Our program involves the synthesis of suitable molecules, tailor-designed to measure intramolecular electron-transfer rates of the type

$$A_1\text{–Sp–}A_2^- \rightleftarrows {}^-A_1\text{–Sp–}A_2 \qquad (1)$$

where A_1 and A_2 are groups with finite electron affinities and Sp is a rigid spacer with no electron affinity of its own. The experiment involves the generation of negative radical ions from the molecules by pulse radiolysis and the kinetic measurement of the intramolecular electron-transfer rates establishing equilibrium by optical absorption. This process is summarized in scheme 2. Of course, *intra*molecular kinetics has to be separated from *inter*molecular reactions by using concentration variation and suitable model experiments.

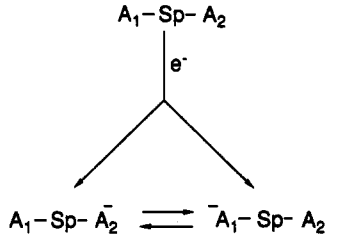

(2)

A few words need to be said to explain the details of the scheme. First, the success of the experiment depends on the ability to generate the two ions in a nonequilibrium distribution. This is the case in all the systems we have examined. It was therefore possible to follow the reactions to equilibrium and determine rate constants. Next, it is important that the electron capture process can be kept fast enough so that is does not become rate determining. This was possible by increasing the concentration of the bifunctional molecule to the point that the bimolecular capture process is faster or comparable to the electron-transfer rate.

The advantage of the pulse radiolysis method to study ET is the fact that ion pairs generated by high-energy radiation are known to have a spatial distribution function for the oppositely charged ions which disfavors tight or contact ion pairs. Furthermore, in the cases we have studied, the counterions are so reactive that the anions disappear on contact with them,[58] further discriminating against close ion pairs. This is important in ET studies because the rates can be controlled by the counterion motion.[59] While this is an interesting subject by itself, it was not the primary aim of our study which focuses on ET in free ions. Equally important is the fact that, at least in principle, it is possible to create ions in any solution including solvents of extremely low dielectric constants such as hydrocarbons.

Having outlined the experiment, we set forth the detailed goals of our study. It is our aim to derive quantitative relationships between the rates of LDET and the following variables: (1) free energy of the reaction (ΔG), (2) solvent, (3) distance, and (4) steric effects. While we have results to report on each of these subjects, the project is by no means complete. For example, at this time we will not cover temperature effects, thus neglecting the important contributions entropy effects may have on the reaction rates. In a way, this paper should be regarded as a progress report on our work.

Free Energy and Solvent Effects

The molecular system we have chosen to study these effects makes use of the well-known geometry and rigidity of the steroid molecules, providing us with an almost ideal spacer as defined above. Attachment of the electron acceptors at positions 3 and 16 of the 5-α-androstane skeleton with β stereochemistry gives an edge-to-edge distance of 10.3 Å. Specifically, the series of eight molecules constructed for this study is represented by **1** containing

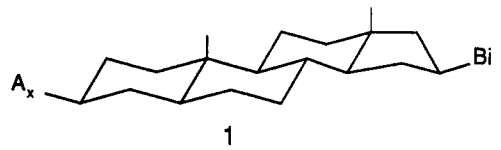

1

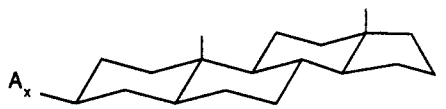

2

a 4-biphenyl substituent at 16-β and eight different acceptors (A_x) at 3-β. The acceptors are listed in Table I, and structures are shown in Figure 1. These acceptors were chosen to have a larger electron affinity than biphenyl and cover a range of electron affinities of almost 2.4 eV. The rates to be compared involve electron transfer from the biphenylyl group to the acceptor at position 3.

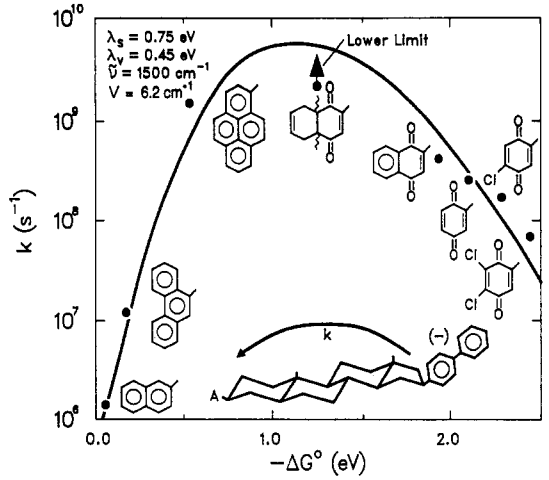

Figure 1. Intramolecular ET rate constants of the negative ions of the compounds listed in Table I as a function of free energy change in MTHF at 296 K. Electrons are transferred from the 4-biphenylyl ion group to the acceptors (A_x) having the general structures shown.

To obtain the desired intramolecular ET rate constants, solutions of these compounds in three different solvents, 2-methyltetrahydrofuran (MTHF), tetrahydrofuran (THF), and isooctane at room temperature were subjected to a high-energy (20 MeV) electron pulse from the Argonne Electron Linear Accelerator while monitoring the absorption spectrum of the solution. Depending on the expected rate constants, electron pulses of either a few nanoseconds or 30 ps duration were used. The absorption measurements were made in standard ways using either vacuum (biplanar) or solid-state photodiode detection. In most cases the absorption decay of the anion of the biphenylyl group was monitored at 400 or 650 nm, and in some favorable cases the growth of absorption of the final acceptor was also measured. The rates of electron capture by the bifunctional molecules was determined independently by monitoring the decay of the solvated electron at 1000 nm. Finally, the experiments were repeated at several concentrations of the bifunctional molecules. This was necessary to sort out the intramolecular ET from the intermolecular component. Monofunctional model compounds **2** were also synthesized for all A_x, and the rates of their intermolecular reactions with the monofunctional 4-biphenyl anion (**2**, A_x = 4-biphenyl) were measured independently and served as guides in evaluating the

(58) Jou, F. Y.; Dorfman, L. M. *J. Chem. Phys.* **1973**, *58*, 4715.
(59) Szwarc, M.; Jagur-Grodzinski, J. In *Ions and Ion Pairs in Organic Reactions*; Szwarc, M., Ed.; Wiley: New York, 1974; Vol. 2, p 1.

intermolecular components of the bifunctional molecules.

A few words need to be said regarding the evaluation of the absorbance vs. time data. Pulse radiolysis creates ion pairs rather than single ions because the initial high-energy electrons are few and pass through the sample with almost no loss of their numbers. So the electrons which attach themselves to the acceptors originate from the solvent and therefore leave a corresponding number of positive "holes". The possibility of hole–negative ion reactions complicates the evaluation of the data. This becomes particularly severe when one is looking at very short time scales where geminate ion recombination becomes a major problem. We have dealt with this in an empirical way. That is, we have determined geminate decay rates by measuring the decay rate constants of the appropriate monofunctional derivatives at various concentrations. By building those decays into our computer program used for evaluating the kinetics, we have allowed for decay by geminate recombination. A description of the kinetics treatment is given in the Appendix.

Next, it was necessary to know the initial distribution of the two ions produced by electron capture at either end of the bifunctional molecules. This can be achieved by measurements of the absorption shortly after the electron pulse at two different wavelengths, preferably chosen to give maximum differences for the absorbancies of the two ions. Of course, this requires the knowledge of the relative extinction coefficients of the two ions. This information is available from the corresponding monofunctional model compounds. In all cases included in the series the ratio of the initial formation of the two ions was very close to unity.

The intramolecular ET rates measured in the steroid series in methyltetrahydrofuran at room temperature are listed in Table I together with the corresponding intermolecular rates. The results are plotted against the free energies of the reactions in Figure 1. The free energy changes for the first two reactions with 2-naphthyl and 9-phenanthryl accetors were determined directly by measuring the ion equilibria with the pulse radiolysis method. For the remaining acceptors this was not practical, and the values were obtained from electrochemical data in the literature. Due to not strictly comparable solvent and electrolyte effects, there is a larger uncertainty associated with these values, but we estimate the errors not to exceed 0.1 eV. It is significant that the equilibria measured directly in our pulse radiolysis experiments differ from the corresponding electrochemical data by less than 20 mV in free energy. The values of ΔG are listed in Table I.

Inspection of the data immediately reveals an initial rise of the rates with increasing exoergicity followed by an "inverted region"[60] where further increase of the driving force leads to a decrease in rate. While there have been isolated examples[61-63] hinting at the possible existence of an inverted region, we believe this to be the first unambiguous demonstration for reactions in liquid solution of the rate–free energy relationship predicted by Marcus almost 30 years ago.[60] *The behavior shown in Figure 1 represents a dramatic deviation from the classical Bronstedt relationship and all the other linear free energy relationships which have been so successful in physical organic chemistry over the past 50 years!*

At this point it becomes necessary to relate our data to theory. From the multitude of existing electron-transfer theories we have chosen the nonadiabatic theories developed in the 1970s.[64-75] These theories are reasonably simple but adequate for most experiments. They describe LDET as an activated radiationless transition, thus relating it to the golden rule expression

$$k = (2\pi/\hbar)|V|^2\mathrm{FCWD} \tag{3}$$

in which the rate is treated as the product of an electronic part containing the coupling matrix element, V, and the Franck–Condon weighted density of states (FCWD). The evaluation of the latter is done with a semiclassical model in which the solvation is treated as a continuum of states and the donor state is assumed to be the vibrational ground state while quantized vibrational states of the acceptor portion of the molecule are specifically included. For simplicity the original Marcus assumption[60] of a double parabolic potential for the solvation energy of the ions has been retained. Also, it is assumed that the relevant vibrations can be approximated by one averaged mode resembling carbon skeletal motions of the acceptor molecular fragment.[23,68,71] With this the expression for the rate of LDET can be written as

$$k = (\pi/\hbar^2\lambda_s k_B T)^{1/2}|V|^2\sum_{w=0}^{\infty}(e^{-S}S^w/w!)\exp\{-[(\lambda_s + \Delta G + wh\nu)^2/4\lambda_s k_B T]\} \tag{4}$$

$$S = \lambda_v/h\nu \tag{5}$$

where S is the vibrational–electronic coupling strength, which is a simple function of reduced bond length changes. The total reorganization energy, λ, is broken up into its solvational, λ_s, and vibrational components, λ_v. The relationship between (3) and (4) is clearly apparent if the summation in (4) is considered to be the relative Franck–Condon factor. The solid line in Figure 1 represents the best fit of k as calculated by (4) to the experimental data. The fit involves the adjustment of two parameters, λ_v and λ_s, and the coupling matrix element V, which functions as a scaling factor. A few additional comments may be needed to justify the fitting procedure. First, the vibrational frequency of 1500 cm^{-1} has been chosen to be compatible with experimental observations[70] which clearly implicate skeletal vibrations as being mostly involved in ion formation. The high-frequency hydrogen modes seem to be of lesser importance. Of course, we are fully aware of the fact that treating a complicated system like ours with a one-mode model is a drastic simplification which makes the separation of the rate into electronic and nuclear coordinate factors less rigorous than a more complete model would. However, this is all we can do in the absence of specific experimental information on those other vibrational modes. In addition, we do not believe that this simplification has more than a quantitative effect on the interpretation of the data. A more dubious procedure is the treatment of the whole series of molecules with constant reorganization energies, λ_s and λ_v. This simplification would be more justified if the series had only aromatics of similar size as the acceptor portions of the molecules. As it is, the five most exoergic points involve quinone-type molecules in which the charge is probably more localized than in the hydrocarbon fragments of the molecules constituting the less exoergic part of the series. Presumably, greater localization of charge leads to larger reorganization energies. Unfortunately, the change in solvation energies throughout the series is hard to estimate quantitatively. Rather than adjusting a parameter in a more or less arbitrary fashion, we prefer to deal with this problem in the cavalier fashion of ignoring it. However, we feel it important to emphasize the fact that if the quinones did not have a larger reorganization energy, the rate falloff at larger exoergicities would be even more pronounced. Thus, the

(60) Marcus, R. A. *J. Chem. Phys.* **1956**, *24*, 966.
(61) Creutz, C.; Sutin, N. *J. Am. Chem. Soc.* **1977**, *99*, 241.
(62) Jonah, C.; Matheson, M. S.; Meisel, D. *J. Am. Chem. Soc.* **1978**, *100*, 449.
(63) Wallace, W. L.; Bard, A. J. *J. Phys. Chem.* **1979**, *83*, 1350.
(64) Levich, V. O. *Adv. Electrochem. Electrochem. Eng.* **1966**, *4*, 249.
(65) Dogonadze, R. R. In *Reactions of Molecules at Electrodes*; Hush, N. S., Ed.; Wiley-Interscience: New York, 1971.
(66) Grigorov, L. N.; Chernavskii, D. S. *Biophysics (Engl. Transl.)* **1972**, *17*, 202. Blumenfeld, L. A.; Chernavskii, D. S. *J. Theor. Biol.* **1973**, *39*, 1.
(67) Hush, N. S. *Trans. Faraday Soc.* **1961**, *57*, 577.
(68) Kestner, N. R.; Jortner, J.; Logan, J. *J. Phys. Chem.* **1974**, *78*, 2148.
(69) Webman, I.; Kestner, N. R. *J. Chem. Phys.* **1982**, *77*, 2387.
(70) Van Duyne, R. P.; Fischer, S. F. *Chem. Phys.* **1974**, *5*, 183.
(71) Fischer, S. F.; Van Duyne, R. P. *Chem. Phys.* **1977**, *26*, 9.
(72) Ulstrup, J.; Jortner, J. *J. Chem. Phys.* **1975**, *63*, 4358.
(73) Newton, M. D. *Int. J. Quantum Chem., Quantum Chem. Symp.* **1980**, *14*, 363. Brunschwig, B. S.; Logan, J.; Newton, M.; Sutin, N. *J. Am. Chem. Soc.* **1980**, *102*, 5798.
(74) Jortner, J. *J. Chem. Phys.* **1976**, *64*, 4860.
(75) (a) Dogonadze, R. R.; Kuznetsov, A. M.; Vorotyntsev, M. A.; Zakaroya, M. G. *J. Electroanal. Chem.* **1977**, *75*, 315. (b) Dogonadze, R. R.; Kusnetsov, A. M.; Vorotyntsev, M. A. *Z. Phys. Chem. (Munich)* **1976**, *100*, 1.

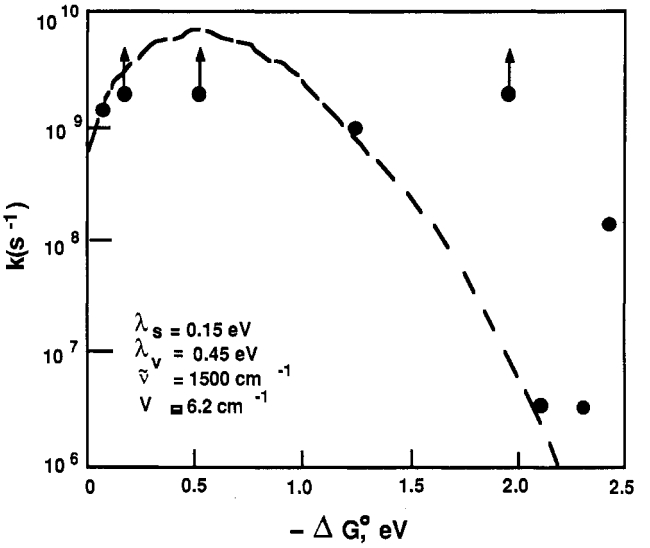

Figure 2. Intramolecular ET rate constants as a function of free energy change in isooctane at 296 K. The points correspond to the compounds with the same A_x groups shown in Figure 1 following the same sequence along the free energy axis.

uncertainty of the solvation energies does not in any way detract from the major conclusions reached from this experiment. Another tacit assumption in the treatment of the data is that the coupling matrix element is constant throughout the series. While we know this not to be strictly true, we believe the variations to be minor. Our present data do not support or deny our belief, and therefore we intend to address this point with experiments in the near future.

Inspection of eq 4 shows that the rate goes through a maximum when the free energy of the reaction approximates the sum of the solvation and vibrational reorganization energies. While the vibrational component within a given series cannot be changed, it is possible to alter the solvational reorganization energy drastically by changing the solvent polarity. For example, a switch from MTHF, a mildly polar solvent, to hydrocarbons would reduce λ_s by a large amount and consequently would shift the rate maximum to much smaller exoergicities. The pulse radiolysis method allows us to do this experiment, and Table I lists the intramolecular ET rates for the same eight compounds in isooctane. Figure 2 shows the results plotted in the same way as the MTHF data. In line with the prediction, it is clear that the rates of the compounds with small driving force have accelerated tremendously, as much as 3 orders of magnitude, while some of the highly exoergic reactions have slowed down substantially. Unfortunately, some of the data points are only lower limits because the rates have become too fast for us to measure. Also, it is apparent that two of the quinones, naphthoquinone and 2,3-dichloroquinone, are not following the predicted behavior. However, these exceptions can be readily explained although we do not yet have experimental proof: When the reaction becomes very exoergic, it is possible for electron transfer to yield an electronic excited state of the acceptor moiety. There is ample precedent for chemiluminescence on radical ion annihilation, for example. This reduces the apparent exoergicity of the reaction, leading to very high rates in the present example. If the initial ion state is poorly solvated, the possibility of excited-state formation is increased because of the decreased activation for this reaction mode. From the absorption spectra of the corresponding ions we know that there is enough energy to populate the excited states of the compound which fall off the line. It may well be that the 5-chloroquinone derivative leads to a small fraction of excited state as well. Unfortunately, negative radical ions of the type we are dealing with are known to have almost zero fluorescence quantum yields, and we will have to use other means to support this explanation in future experiments. Nevertheless, the drastic rate increase observed for the first few points and the observed slowdown for quinone and chloroquinone are perhaps even more spectacular evidence in support of the original Marcus theory than the existence of an inverted region. If our interpretation of the two badly behaved points is correct, the inverted region now covers most of the free energy span.

There are far-reaching consequences of the solvent effect described by the comparison of Figures 1 and 2. Much attention has been paid to the subject of photochemical charge separation in recent years.[8-10] It has become apparent that after the initial charge separation step it is important to move the negative charge away from the donor hole as fast as possible. Also, it is important to preserve as much of the free energy of the exciting photon as possible and to prevent the occurrence of the energy-wasting back-reaction. With these requirements it becomes obvious that an efficient charge-separating machine has to work under conditions represented by Figure 2 rather than Figure 1. One wants to maximize the rate with low driving force and minimize it for the much more exoergic back-reaction. Those conditions are better described by Figure 2. To put it differently, to maximize the efficiency of photosynthesis, one should work in "oil and not in water". It is gratifying to have learned over the past few months that the protein surrounding the charge separation complex used by photosynthesizing bacteria is devoid of charged components, thus providing a relatively nonpolar environment.[43]

Finally, one may ask why it took so long to verify experimentally the Marcus inverted region. Of course, we do not know the answer, but we have a suggestion. As pointed out in the Introduction, intermolecular ET is composed of two steps, diffusion and electron transfer. The most influential work designed to test the Marcus prediction is that of Rehm and Weller.[76] They studied intermolecular ET over a large range of exoergicities. All they found was an initial rise followed by a plateau without an inverted region. The most likely explanation is that when reaching the plateau the reactions became diffusion controlled and what was measured was no longer the ET rates but rather diffusion rates. Also, in the region of extremely exoergic reactions there were many compounds included that can form excited states. How diffusion masks free energy effects is most dramatically shown when the *inter*molecular rates corresponding to our steroid series are compared over the whole free energy region (Table I). Instead of observing several orders of magnitude differences, all that remains is a factor of 4, hardly worth reporting!

At this point it should also be mentioned that the experiments in liquid solution presented here were a logical follow-up of experiments done in rigid matrices which provided the first example of the existence of an inverted region.[23,24,75]

Distance Dependence and Stereoelectronic Effects

As has been pointed out above, we have assumed that the electronic coupling between donor and acceptor fragments is approximately constant throughout the steroid series. Therefore, the observed rate variations have been attributed to the nuclear coordinates giving rise to a variation in the Franck–Condon factors. In this section we wish to describe our attempts to gain insight into the electronic coupling. To do this, one wants to change the coupling matrix element, V, while keeping the Franck–Condon factors as constant as possible. It is usually assumed that within the limit of weak coupling, as is appropriate for nonadiabatic ET, the matrix element, V, as defined by (6) should fall off expo-

$$\langle A_1^{-}\text{-Sp-}A_2|\mathbf{H}|A_1\text{-Sp-}A_2^{-}\rangle = V \qquad (6)$$

nentially with donor–acceptor distance (R_{DA}) as shown in (7)

$$V = V_0 \exp\{-[\beta(R_{DA} - R_0)/2]\} \qquad (7)$$

where the attenuation is given by β and R_0 is the distance at the van der Waals radius. This assumption is reasonable for the case where donor and acceptor are separated by empty space, considering the distance dependence of the tail of the wave function. But even in this ideal case there should also be an orientation dependence for all molecules which are not spherically symmetric. Indeed, recent calculations by Siders, Cave, and Marcus[77] have

(76) Rehm, D.; Weller, A. *Isr. J. Chem.* **1970**, *8*, 259.
(77) Cave, R. J.; Siders, P.; Marcus, R. A. *J. Phys. Chem.*, in press.

TABLE II

Compound	Symbol	# of Bonds	# of Isom	Compl
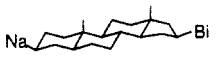	Ste	10	---	✓
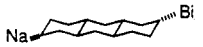	A-2,8	9	4	
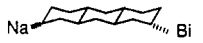	A-2,9	8	4	
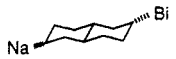	D-2,6	7	4	✓
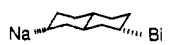	D-2,7	6	4	✓
	C-1,4	5	2	✓
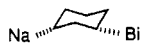	C-1,3	4	2	✓
	C-1,2	3	2	
	M	2	1	

predicted such anisotropies. These orientational effects leave the exponential distance dependence intact but lead to a variation in V_0. However, in intramolecular LDET it becomes questionable whether an exponential falloff with distance can form the basis of a realistic model. While the electron density on the spacer portion of the molecule is certainly extremely small, it appears quite reasonable to assume that the spacer plays a specific role in transmitting the coupling between donor and acceptor. One should expect the number and types of bonds and their mutual geometry to enter into the expression for the exponent rather than just a distance dependence. Orientational effects leading to variations in coupling of the donor and acceptor to the spacer will lead to changes in the preexponential factor. Of course, these suggestions are not new and there have been both theoretical and experimental verifications of these concepts.[11,78-84] Nevertheless, quantitative data are sparse and we hope that our studies might help to shed some light on the problem.

The guiding principle of our experimental approach has been to design and construct a series of molecules of the type **1** where we keep the donor–acceptor pair constant but vary the spacer in a systematic manner. The size and nature of the spacer will determine the coupling while the Franck–Condon factors, which are mainly determined by the donor–acceptor pair, hopefully do not change very much except for the distance dependence of the solvation reorganization energy which can be partly corrected for. The series decided upon is shown in Table II and has the following features. First, the steroid nucleus is the largest spacer and a single saturated carbon atom is the smallest. If one uses a bond count along the shortest pathway between donor and acceptor as a measure, the series covers a range from 10 to 2 bonds. Next we have chosen the biphenyl–naphthalene (Bi–Na) pair because it is the slowest in the steroid series and we did not want to run into reactions too fast to measure (although we did). Also, the small free energy of the reactions allowed us to measure this quantity

(78) See examples and references in the following two reviews.
(79) Marcus, R. A.; Sutin, N. *Biochim. Biophys. Acta* **1985**, *811*, 265.
(80) Newton, M. D.; Sutin, N. *annu. Rev. Phys. Chem.* **1984**, *35*, 437.
(81) Stein, C. A.; Lewis, N. A.; Seitz, G. *J. Am. Chem. Soc.* **1982**, *104*, 2596.
(82) Beratam, D. N.; Omuchic, J. N.; Hopfield, J. J. *J. Chem. Phys.* **1985**, *83*, 5325.
(83) Larsson, S.; Matos, J. M. O. *J. Mol. Struct.* **1985**, *120*, 35.
(84) Hale, P.; Ratner, M. A. *Int. J. Quantum Chem., Quantum Chem. Symp.* **1984**, *18*, 195.

TABLE III

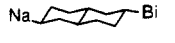	D-2,6-ee	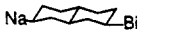	D-2,7-ee
	D-2,6-ea	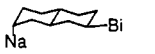	D-2,7-ea
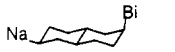	D-2,6-ae	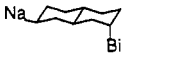	D-2,7-ae
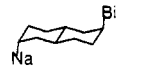	D-2,6-aa	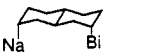	D-2,7-aa

TABLE IV: Distances, Rate Constants, and Coupling Matrix Elements of Compounds with 4-Biphenyl-2-Naphthyl Donor–Acceptor Pairs

compd	$(R_{DA})_{center}$,[a] Å	$(R_{DA})_{edge}$,[a] Å	k,[b] s^{-1}	λ_s, eV	V, cm^{-1}
Ste	17.4	10.3	1.5×10^6	0.75	6.2
D-2,6					
ee	14.0	6.7	5.0×10^7	0.72	34
ea	11.4	6.3	5.9×10^7	0.67	26
ae	11.0	6.3	2.3×10^7	0.66	15
aa	11.9	6.1	5.8×10^7	0.68	27
D-2,7					
ee	12.5	6.4	2.9×10^8	0.69	63
ea	11.4	6.0	3.0×10^8	0.67	58
ae	10.9	6.0	1.75×10^8	0.66	42
aa	6.2	5.3	25×10^8	0.47	58
C-1,4					
ee	11.8	4.4	1.6×10^9	0.68	141
ea	9.5	4.0	2.5×10^9	0.62	129
ae	9.3	4.0	0.45×10^9	0.62	55
C-1,3					
ee	10.0	3.8	4.2×10^9	0.64	185

[a] Measured from distances optimized by molecular mechanics, MM-2 calculations. [b] Error limits estimated to be ±25%, and ±40% for rates in excess of 10^9 s^{-1}.

directly by measuring equilibria under our reaction conditions, thus eliminating one uncertainty in the interpretation of the data. Last, but not least, this donor–acceptor pair gave us the least problems with the synthesis. Looking at the series, it becomes immediately obvious that another advantage is the existence of four stereoisomers for each of the carbon skeletons. The type of isomers encountered is shown in Table III for the decalin series. While this aggravated the synthetic problem, it gave us an opportunity to examine stereoelectronic effects of the kind which had not been looked at before. Unfortunately, the series is not complete at the time of this writing, but some significant features have already emerged from the available data.

Table IV lists the intramolecular rate constant obtained in THF for LDET in the 13 compounds for which data are available at the time of this writing. It is obvious from inspection that as the distance between donor and acceptor decreases, the rate goes up. A more informative evaluation of the data is obtained by plotting the logarithms of the rates against distance. Immediately, such an effort leads to the important question: What distance? It is necessary to define distances which in the case at hand are comparable to the size of the donor–acceptor portions of the molecules. One way to do this is to define center-to-center distances which have been used successfully before. Figure 3A shows a logarithmic plot of the rate constants against these center-to-center distances. The next approach is to consider the beginning of the π-electron skeleton of donor and acceptor as the relevant distance. This so-called edge-to-edge distance, measured from the center of the σ bond of the donor to the center of the acceptor attachment bond, is plotted in Figure 3B. Finally, it makes sense to plot the rates against the number of intervening σ bonds. Such a plot is shown in Figure 3C. It is obvious that none of the plots are very satisfactory for a linear correlation.

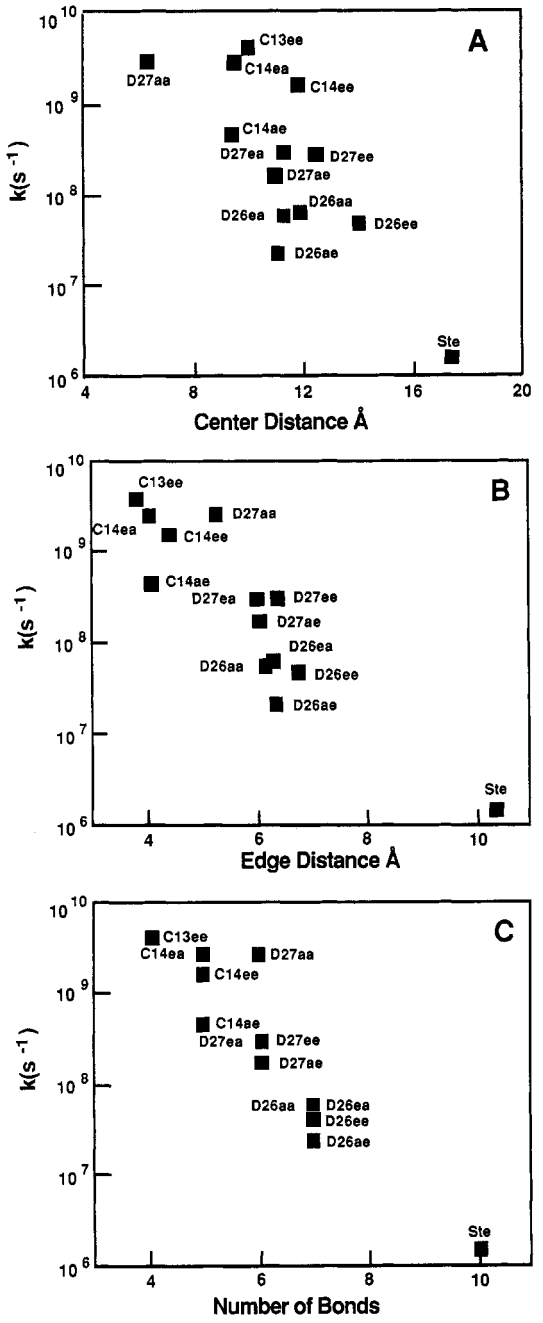

Figure 3. Intramolecular ET rates for the negative ions of the compounds listed in Tables II and III in THF at 296 K plotted against (A) center-to-center distance, (B) edge-to-edge distance, and (C) minimum number of intervening σ bonds.

At this point it became apparent that distance or even number of bonds, while important, are not the only factors determining the ET rates and that steric factors should not be neglected. Specifically, axial vs. equatorial attachment to the cyclohexane rings might play an important role. Directly related to this problem are the rotational conformations of the aromatic groups relative to the spacer framework. To discuss this problem, we have to examine the basic stereochemistry of our compounds and make use of ab initio MO calculations carried out in collaboration with Ohta and Morokuma[85] and which were prompted by the experimental results.

In all our compounds, with the exception of the 16-substituent of the steroid series, the donors and acceptors are attached to a cyclohexane ring which makes it possible to have equatorial or axial conformations as shown in Table III. An additional degree of freedom of considerable importance is the angle defining the

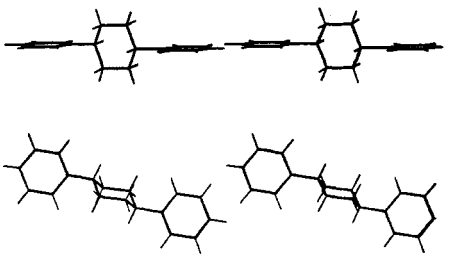

Figure 4. VERSORT drawings of side and end views of *trans*-1,4-biphenylcyclohexane as determined by single crystal X-ray crystallography. (Structure determination was by J. C. Huffman, Indiana University Molecular Structure Center.)

orientation of the aromatic system relative to the spacer skeleton. This orientation is most conveniently defined by the dihedral angle between the aromatic ring plane and the C–H bond at the attachment position of the cyclohexane ring. A Newman projection (3) with the definition of the dihedral angle, θ, is shown. Two questions arise in connection with this stereochemical analysis. First, what angle corresponds to the energy minimum, and second, what is the magnitude of the coupling element as a function of that angle?

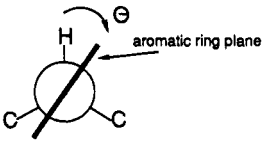

3

The first question can be answered fairly unambiguously by using several methods. An aromatic substituent such as phenyl or biphenyl when attached to a cyclohexane ring in an equatorial stereochemistry prefers the dihedral angle as defined above to be close to 0° (<5°). In other words, the aromatic ring plane prefers to sit nearly perpendicular to the average plane of the cyclohexane ring. This conclusion is reached on the basis of molecular mechanics calculations of the MM-2 type, ab initio or semiempirical MO calculations and, most importantly, from X-ray structure determination on *trans*-1,4-diphenylcyclohexane, a VERSORT drawing of which is shown in Figure 4. However, an axial aromatic substituent on a cyclohexane ring does prefer a dihedral angle as defined above of 55°. Once again this is confirmed by molecular mechanics and MO calculations. This rotamer conformational analysis has considerable consequences on the magnitude of the predicted coupling between donor and acceptor through cyclohexane-type spacers, as revealed by the ab initio MO calculations. The calculations were carried out on a simplified model, 1,4-dimethylenecyclohexane radical anion (A), which should reproduce, certainly in a qualitative way, the more important stereoelectronic effects in our series.

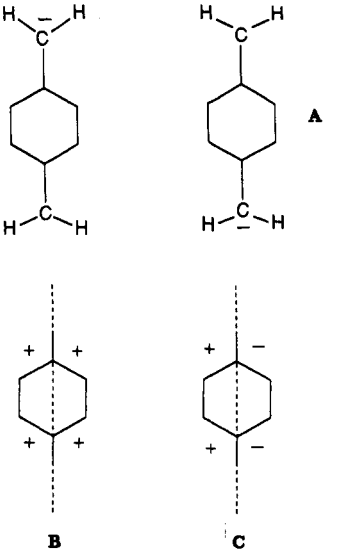

(85) Ohta, L.; Closs, G. L.; Morokuma, K.; Green, N. *J. Am. Chem. Soc.* **1986**, *108*, 1319.

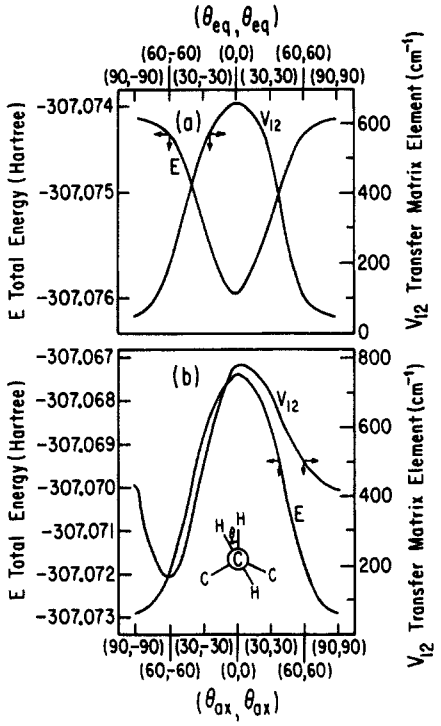

Figure 5. Total energy E (hartree) and coupling matrix element V_{12} (cm^{-1}) of the rotamers shown on the x axis for the ee (a) and aa (b) conformations of *trans*-1,4-dimethylenehexane radical anion. Reproduced from ref 85.

Considering the symmetry of 1,4-disubstituted cyclohexane, it is possible to divide the σ orbitals of the cyclohexane ring into a symmetric (B) and a antisymmetric (C) set with respect to a symmetry plane normal to the ring plane and including carbons 1 and 4. The π systems attached to those carbon atoms will interact more or less strongly with one set or the other, depending on the dihedral angles at those positions. For example, it should be clear that a 0,0 conformation will lead to maximum interaction via the antisymmetric spacer orbitals while the 90,90 conformation will make maximum use of the symmetric set. A 0,90 conformation will, in first order, give no interaction at all. Of course, these arguments presuppose perfect symmetry.

The magnitude of the interaction at any given rotamer conformation will be a function of which kind of orbital set of the spacer will be promoting most efficient mixing between donor and acceptor orbitals. This question cannot be answered by inspection, and we make use of the MO calculations in which the electronic coupling matrix elements and energies were computed for the various dihedral angles. The results are shown in Figure 5 and can be summarized as follows: It appears that for both equatorial–equatorial and axial–axial substitution patterns the interaction matrix element reaches a maximum for the 0,0 rotamer. For each case the 90,90 conformation provides distinctly less coupling. However, this difference is particularly pronounced for the bis-equatorial case where the difference between maximum (0,0 rotamers) and minimum coupling (90,90 rotamers) is almost a factor of 15, while in the bis-axial geometry it is only a factor of 2. It is also noteworthy that the values for maximum coupling for the bis-equatorial and bis-axial cases are very comparable. The behavior of the equatorial–axial conformations is more complicated and will not be discussed here except to note that the interaction for any rotamer angles does not exceed one-third of that calculated for the aa and ee cases. From these calculations it can be deduced that the orbitals interacting the most with the equatorial substituents are antisymmetric with regard to the ring plane. The bis-axial substitution pattern still leads to a preference for the antisymmetric orbital mixing, but in this case the symmetric orbitals are more efficient in providing coupling than they are for bis-equatorial substitution. And in line with the qualitative arguments presented above, the coupling goes to a minimum for 0,90 geometries regardless of the substitution pattern.

While the numerical results are dependent on the basis set used, the qualitative behavior is the same for all basis sets and makes a strong case for the importance of the spacer orbitals in transmitting coupling. The calculations draw attention to the existence of substantial stereoelectronic effects in LDET. In fact, if the cyclohexane is left out altogether, the matrix element takes on a very small value.

We will now discuss the data of Table IV in terms of the coupling analysis of the MO calculations. First, we make the assumption that the 1,4-cyclohexane coupling scheme can be extended to include both decalin systems as well. This is not necessarily justified but is the best we can do at the present time, particularly since the decalin system becomes a little too large for ab initio MO calculations. We did however perform MM-2 calculations for all the compounds in the series, confirming that the dihedral angles for equatorial and axial substituents in the decalins are strictly equivalent to those in the cyclohexanes. Since equatorial substitution leads to an unambiguous rotamer preference near 0° in the whole series, it stands to reason to take all equatorial–equatorial isomers as a standard in which the maximum through-bond coupling is realized. If we include the steroid in this series, there are five such points in our data. Their coupling to the spacer should be all comparable and the ET rates of these compounds should depend on the number of bonds separating donor and acceptor if the coupling is strictly of the through-bond type. This is shown in Figure 6C, showing only the equatorial–equatorial isomers. Indeed, the plot shows a fairly good linear relationship. In Figure 6B the rates for the e,e isomers are plotted against edge-to-edge distance, emphasizing the greater importance of the number of bonds over distance. The sharp change in rate going from 1,3- to 1,4-cyclohexanes and from 2,7- to 2,6-decalins is due to the fact that those changes do not alter the distance very much but, of course, increase the number of bonds by one. Finally, a center-to-center distance plot is shown in Figure 6A, again emphasizing only the equatorial–equatorial isomers. The good fit obtained for this plot is partly accidental and can be traced to the fact that for large substituents the center-to-center distances change much more than edge distances in going from a linear geometry as in a 1,4-substituted cyclohexane to a bent one as in 1,3-cyclohexanes. The same relationship holds for the corresponding decalins.

Before proceeding any further with the analysis of the data, we should recall that the Franck–Condon factors cannot be constant throughout the series, because the solvent reorganization energy is a function of the acceptor–donor distance. While this has no significant effect when this distance is large, substantial changes can be expected for some members of the series such as D-2,7-aa in which the distance is particularly short. This effect has been recognized before,[60] and we will make use of eq 8 to

$$\lambda_s = e^2\{(2r_D)^{-1} + (2r_A)^{-1} - (R_{DA})^{-1}\}(\epsilon_s^{-1} + \epsilon_{op}^{-1}) \qquad (8)$$

correct for it. Here r_D and r_A are the radii of the donor and acceptor, R_{DA} is the donor–acceptor center-to-center distance, and ϵ_s and ϵ_{op} are the static and optical dielectric constants of the solvent, which for THF are available from literature data.[86] Using $\lambda_s = 0.75$ eV as determined for the steroid data and $R_{DA} = 17.3$ Å, we can solve for $(2r_D)^{-1} + (2r_A)^{-1}$. the value obtained, 0.338, corresponds to 2.95 Å for the case $r_D = r_A$ and is quite realistic. With this result we calculated λ_s for each of the compounds in the series, and they are listed in Table IV. Having obtained the coupling matrix element for the steroid series as 6.2 cm^{-1} by fitting the data to eq 4, we can now use the measured rate data to calculate V for all the compounds. This, of course, assumes that other contributions to the Franck–Condon factors are the same for all compounds of the biphenyl-2-naphthyl series.

The values of V are plotted on a logarithmic scale in Figure 7 against center-to-center (A) and edge-to-edge distance (B) and against the minimum number of intervening bonds (C). Again

(86) *Lange's Handbook of Chemistry*, 12th ed.; Dean, J. A.; Ed.; McGraw-Hill: New York, 1969; Chapter 10.

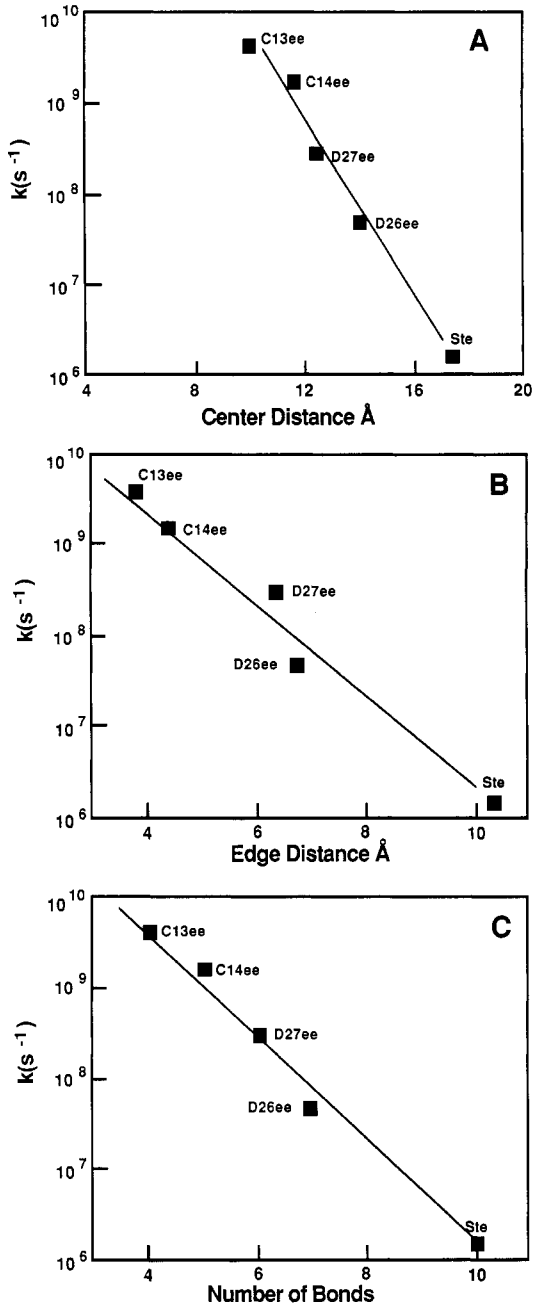

Figure 6. Intramolecular ET rates for the negative ions of the compounds listed in Tables II and III with ee type of attachments against (A) center-to-center distance, (B) edge-to-edge distance, and (C) minimum number of intervening σ bonds.

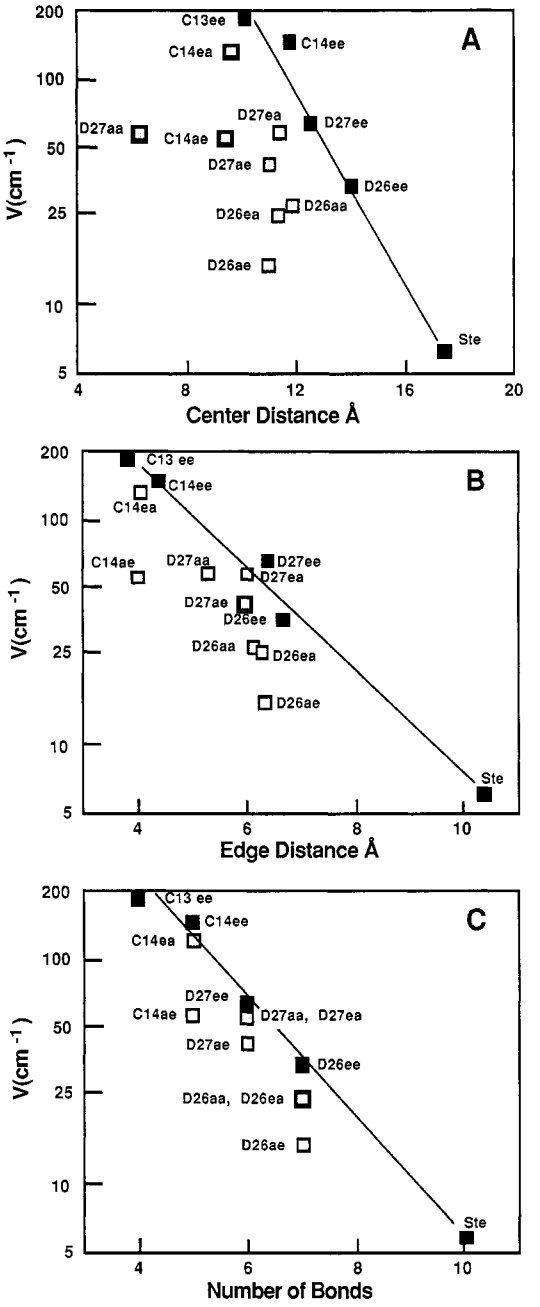

Figure 7. Plot of the coupling matrix element, V^2, as obtained from eq 4 and the experimental rates for the negative ions of the compounds listed in Tables II and III against (A) center-to-center distance, (B) edge-to-edge distance, and (C) minimum number of intervening σ bonds.

the equatorial–equatorial isomers are emphasized and used to form linear correlations.

We will use the center–center distance plot of the bis-equatorial isomers as the basis for a distance correlation although this is a

$$2 \ln V = 2 \ln V_0 - \beta(R_{DA} - R_0) \qquad (9)$$

somewhat arbitrary procedure because as the discussion of the MO calculations above and further examination of the data clearly show most, if not all, of the coupling proceeds through bonds. Again, this is emphasized by the poorer fit to the edge-to-edge distances. Therefore, this correlation is mostly done for the purpose of comparison with other data. The best fit through the data yields $\beta = 1.01$ Å^{-1} at an assumed $R_0 = 6$ Å, $V_0 = 1.9 \times 10^3$ cm^{-1}. A comparison of these values with those obtained for intermolecular ET in rigid glasses shows that the exponential attenuation with distance is approximately 20% less ($\beta_{glass} = 1.21$ Å^{-1}) and V_0 is 6 times as large ($V_{0,glass} = 3 \times 10^2$ cm^{-1}).

This corresponds to a much stronger coupling for the intramolecular systems as is expected if we are observing through-bond interactions. Therefore, it may be more meaningful to establish a correlation with the number of bonds as is shown in (10) which

$$2 \ln V = 2 \ln V_0 - \beta'(\text{no. of bonds} - 1) \qquad (10)$$

is defined to set the one-bond coupling as the limit. The best fit to the bis-equatorial compounds as shown in Figure 7C gives $\beta' = 1.15$ bond^{-1} and $V_0 = 1.1 \times 10^3$ cm^{-1}. The values for V_0 obtained by the two different correlations correspond to a rate difference of a factor of 3 at the minimum distance or number of bonds. Considering that the distance extrapolation to 6 Å is somewhat arbitrary, this agreement is very good. A way of summarizing the two correlations is to state that the rate in these systems should change by a decade every 2.3 Å or every 2.0σ bonds for constant Franck–Condon factors if and only if the attachments of both donor and acceptor to the cyclohexane rings are the same throughout the series. It should be pointed out that the reason the distance and bond correlations are approximately parallel is no accident because of the geometry of our compounds which do not deviate much from linearity, thus assuring that bond number

changes are accompanied by corresponding distance changes. This changes drastically for some of the other conformations shown as nonemphasized points in Figure 7 and which will be discussed now.

Inspection of Figure 7 shows that all the points falling below the lines belong to the axial–axial (aa) and axial–equatorial (ae and ea) isomers. According to the MO calculations (Figure 5), the matrix element for an axial–axial pattern at the equilibrium rotamer conformation of 55,55 is almost as large (80%) as that of the equatorial substitution pattern at 0,0. At 55,–55 however it drops to half that value. If we assume we have a mixture of rotamers, one should expect the aa isomers to be slower than the corresponding ee isomers, but not by much. This is certainly the case for D-2,6-aa and D-2,7-aa which are close to the line of Figure 7C. What is surprising is that D-2,7-aa is not much faster, considering the fact that in some rotamer angles the donor and acceptors are at van der Waals radius. This isomer makes one of the strongest arguments for through-bond interactions winning over through-space interactions. Its position on the distance plot (Figure 7A) emphasizes that argument.

The axial–equatorial isomers correspond to rotamer equilibria describable with dihedral angles of 55,0. Although not shown in the figures, the MO calculations predict a much weaker coupling for this case, less than 30% of the maximum ee coupling. As Figure 7C shows, this prediction is confirmed for D-2,6-ae, D-2,7-ae, and c-1,4-ae, all of which fall substantially below the line. However, the corresponding ea-type isomers are significantly faster than their ae counterparts. This, at first sight, appears to be very puzzling because ea and ae substitution should have the same coupling if the donor and acceptor orbitals were comparable. It was at this point of our study when it became apparent that the choice of 2-naphthyl as one of the substituents might not have been the best one possible. This has to do with the symmetry of the substituents. While 4-biphenylylcyclohexane has a plane of symmetry at 0° and 90° in both equatorial and axial conformations, 2-naphthylcyclohexane has not. Here, only the 0° rotamer, corresponding to the energy minimum for the equatorial substitution, has that symmetry. Therefore, the arguments predicting the magnitude of coupling by symmetry, outlined above, will not hold unless the naphthalene occupies an equatorial position. The problem is aggravated by the fact that the LUMO of naphthalene, which is the important orbital for ET among negative ion radicals, has very different coefficients at the 1- and 3- positions, which are adjacent to the point of attachment. Consequently, the 90° rotamer will couple not only with the symmetric orbitals of the spacer but also with the antisymmetric ones. Therefore, whenever naphthalene is in an axial position, the coupling will be stronger than when the biphenylyl is axial. This somewhat simplisic analysis accounts nicely for the rates of the ea isomers being faster than those of the ae compounds. If correct, acceptors with the same symmetry as 4-biphenylyl should not show this difference.

The 1,4- and 1,3-substituted cyclohexanes have a special problem associated with them due to possible chair-to-chair interconversions. While the bis-equatorial isomers (trans-1,4 and cis-1,3) are essentially one compound because of the much higher energy content of the bis-axial conformation, this is no longer the case for the isomers in which one of the substituents has to be axial at all times (cis-1,4 and trans-1,3). We have determined the equilibrium for the 1,4 isomer by NMR, showing it to be essentially a 1:1 mixture of ea and ae.

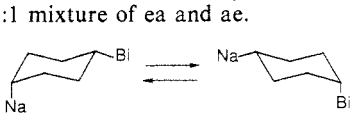

(11)

K = 1.05

The interconversion rates are known to be slow on our time scale (10^2–10^3 s^{-1}). So if ET in ae is much slower than in ea as expected from the decalin results, one would expect strong biexponential behavior for the rates. This was found experimentally. We attribute the slow rate constants to the ae isomers, and for C-1,4 they are listed as such in the Table IV and in the figures. Unfortunately, this complex decay kinetics make the numbers much less certain and an assumption as to the initial ion distribution had to be made. Because of this we have left out the C-1,3-ea and -ae data entirely. But there is no question that the significant difference between ea and ae as noted in the decalins does also exist for the cyclohexanes and is perhaps even more pronounced.

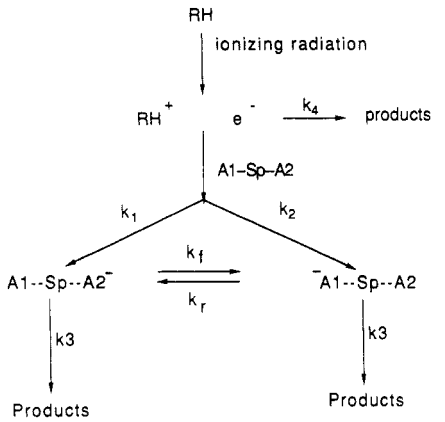

Figure 8. Reaction scheme used for the kinetic analysis of the data.

Each substitution pattern should have its own dependence on numbers of bond between donor and acceptor. Although the data are insufficient to constitute experimental proof, the correlations should differ from (10) only by V_0 and all the isomer series should have the same slope.

Conclusion

As has been stated in the Introduction, this study is incomplete at this point. But we believe we have demonstrated a number of important aspects of electron transfer which were less well understood at the outset of our work. Among these is the demonstration that the Marcus inverted region does exist even for reactions in solutions but can generally only be expected to play a major role when diffusion as the rate-limiting step is eliminated and when transfer to excited states is impossible. The solvent effects demonstrated in this study are large and must be taken into account in any evaluation of ET kinetics. Temperature dependences must be measured to evaluate activation energies and entropies directly. The accompanying viscosity changes will give information on solvation dynamics and may lead to substantial deviation from Arrhenius behavior.

At about the same time we commenced this work several other groups began work on LDET in proteins.[35-42] Among these, the results obtained by the groups headed by Gray, Isied, Hoffman, and McLendon are particularly interesting. Comparison of their rates and ours shows the protein rates to be many orders of magnitude slower. While some of this can be accounted for by the fact that the distances are often very much larger, it cannot entirely explain the differences. In view of the results represented in the second half of this paper, it appears that the absence of the through-bond components in the proteins studied may make a large difference. The bond connectivities in the proteins are much longer than the direct distances imply. In this connection it is interesting to note that, in photosynthetic reaction centers where LDET has to be very fast to compete with excited-state deactivation, nature has provided a "bridging" group between donor and acceptor in the form of an additional chlorophyll molecule. In view of our results, we believe this molecule to function as a bridge for the establishment of a coupling matrix element of the required magnitude.

The stereoelectronic effects discussed in the last part of this paper have, at this point, only been touched upon. However, they are convincing evidence for the through-bond coupling even through saturated hydrocarbons. Besides the lack of appropriate symmetry of the naphthalene acceptor, another shortcoming of our system is the fact that the rotamer potentials are relatively shallow, so that at room temperature the rotamer angles will have a wide distribution around the energy minima. This diminshes the magnitude of some of the predicted effects. Work is in progress to construct molecules with well-defined rotamers in steep potential

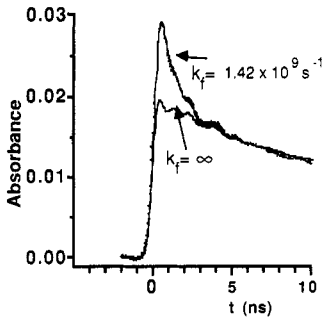

Figure 9. Absorbance vs. time (unconnected points) for a 0.0259 M solution of *trans*-1-biphenyl-4-naphthylcyclohexane (eq,eq) in THF along with a fit giving a forward electron-transfer rate constant, $k_f = 1.42 \times 10^9$ s^{-1} (the solid line through the data). The fitting function was convoluted on the measured system response function to account for risetime and ringing of the detection system. Also shown is the same fit with k_f set to infinity to show how much of the decay of the absorbance is due to the electron-transfer reaction.

wells, and we predict stereoelectronic effects as large as 2 orders of magnitude for specifically designed structures.

Many other aspects of stereochemistry can be exploited. In many ways the problem is related to those associated with long-range electron hyperfine interactions and nuclear spin coupling. Results obtained in these areas may serves as guidelines for some of our future experiments. Lastly, the authors want to express their admiration for the man who predicted so many of our findings long ago: Rudi Marcus!

Acknowledgment. We thank Donald Ficht and George Fox for the high-quality linac beam, Charles Jonah for enlightening discussions on geminate ion kinetics, and W. F. Mooney for assistance in collecting data. G.L.C. is grateful to the Japanese Ministry of Education for financing an extended visit to the Okazaki Institute of Molecular Science where the MO calculations were carried out.

Appendix

This Appendix should help to understand the basis of the least-squares fitting procedure used to evaluate the data. The procedure is based on a reaction scheme shown in Figure 8. Ionization of the solvent (R–H) by the high-energy electrons produces solvated electrons (e_s^-) and solvent cations ($R-H^+$). In subsequent processes the solvated electrons may attach themselves to the bifunctional solute molecules to produce the desired ions. Concurrently, both the electron and the anions may disappear by reactions with the counterions or, more likely, their decompsition products (processes 3 and 4). The electron-transfer rate constants, k_f and k_r, are made up of intra- and intermolecular contributions. To obtain the intramolecular rate constants, solute concentrations should be large enough to make electron attachment to the solute faster than the disappearance of the resulting ions by electron transfer yet low enough that intermolecular transfer is not dominant.

The attachment and decay processes were measured by using model molecules of the type A_1--Sp or A_1--Sp--A_1, in which there is either no electron transfer or no effect of electron transfer on the optical absorbance. The data were fit to the solution obtained by integrating the rate expressions corresponding to the scheme using nonlinear least-squares minimization to obtain k_1, k_2, k_3, k_4, and the extinction coefficients for e_s^-, A_1^-, and A_2^-. Then with all of those parameters fixed, the same procedure was applied to data on bifunctional molecules with k_f and $K_{eq} = k_f/k_r$ as the only adjustable parameters to be obtained from the fit of the model to the data.

Because most of the electrons and ions produced decay geminately with products formed from counterions, the decay processes follow no simple kinetic order. Over a limited range of time (2–3 decades), it is adequate to fit the decays to a sum of 2–3 exponentials each. Our procedure uses three k_3's and three k_4's obtained from fits to the models.

For processes occurring during a few nanoseconds or less, the optical absorbance transients are strongly affected by the system risetime (0.7 ns) and by ringing of the detector. The system response was routinely measured by using 30-ps Cerenkov light pulses from the linac. The measured system response function was then iteratively convoluted with the solution of the reaction scheme.

The method employed here rests on the assumptions that electron attachments and transfer processes may be described as single exponentials and that the decay processes can be simulated with two or three exponentials which are the same for the two ions. In addition, for the very fast ET rates ($k_f > 2 \times 10^9$ s^{-1}), k_f is not uniquely determined by the procedure unless we make an assumption about the electron capture ratio by the bifunctional molecules. A plausible assumption is to set the ratio $k_1/(k_1 + k_2) = 0.5$, a value determined to be correct for the slower reactions. An example of an actual least-squares fit to a set of data is shown in Figure 9.

Registry No. **1** (A_x = 4-biphenylyl), 102683-16-9; **1** (A_x = 2-naphthyl), 102735-05-7; **1** (A_x = 9-phenanthryl), 102735-06-8; **1** (A_x = 1-pyrenyl), 102735-07-9; **1** (A_x = 4a,5,8,8a-tetrahydro-1,4-naphthoquinon-2-yl), 102735-08-0; **1** (A_x = 1,4-naphthoquinon-2-yl), 102735-09-01; **1** (A_x = 2-benzoquinonyl), 102735-10-4; **1** (A_x = 5-chloro-2-benzoquinonyl), 102683-17-0; **1** (A_x = 5,6-dichloro-2-benzoquinonyl), 102735-11-5; A-2,8, 102683-18-1; A-2,9, 102683-19-2; C-1,4, 102683-20-5; C-1,3, 102683-21-6; C-1,2, 102683-22-7; D-2,6-ee, 102683-24-9; D-2,6-ea, 102735-12-6; D-2,6-ae, 102735-13-7; D-2,6-aa, 102735-14-8; D-2,7-ee, 102683-25-0; D-2,7-ea, 102735-15-9; D-2,7-ae, 102735-16-0; D-2,7-aa, 102735-17-1; M, 102683-23-8.